Available online at www.sciencedirect.com

ScienceDirect

Energy Procedia 64 (2015) 73 – 82

Energy Procedia

3rd Trondheim Gas Technology Conference, TGTC-3

Analysis of Natural Gas Engine De-Loading on LNG Fuelled Vessels

Joseph DiRenzo[a,*], Petter Nekså[b], Kjell Kolsaker[a]

[a]Norwegian University of Science and Technology,Høgskoleringen 1, 7491 Trondheim, Norway
[b]SINTEF, Strindveien 4, 7465 Trondheim,Norway

Abstract

Onboard the Norwegian Coast Guard vessel KV Bergen, as well as other LNG fuelled vessels, there has been reports of a sudden fall in the fuel tank system pressure, resulting in de-loading of the NG engines. This study examines the factors which caused the LNG tank pressure on KV Bergen to fall, leading to the de-loading of the Natural Gas (NG) engines. One reason for the drop in tank pressure is that external disturbances from rough seas destroy the liquid surface layer, causing an increase in the rate of condensation occurring inside the tank. The rate of heat and mass transferred to the vapor section by the Pressure Build Up (PBU) unit is less than the heat and mass absorbed during the mixing inside the LNG tank. A process is developed to calculate the possible fall in LNG tank pressure caused by complete mixing of the liquid and vapor.

Peer-review under responsibility of the Scientific Committee of TGTC-3

Keywords: Liquefied Natural Gas (LNG); Tank mixing; Pressure Build Up Unit (PBU), De-loading, Natural Gas (NG) Engine, Norwegian Coast Guard (Kystvakten)

Peer-review under responsibility of the Scientific Committee of TGTC-3
doi:10.1016/j.egypro.2015.01.010

1. Introduction

As emission standards become more stringent and the price of Liquefied Natural Gas (LNG) falls, more vessels are making the decision to switch to LNG as fuel. The Norwegian Coast Guard (Kystvakten) currently maintains three LNG dual fuel vessels in its fleet. Since the use of LNG on vessels other than the large LNG tankers is relatively new, a few engineering problems are still being explored. One documented problem is the unintentional gas engine de-loading event on KV Bergen and other LNG fueled vessels like the Fjord 1 ferries and Eidesvik Shipping resupply vessels. The objective of this study is to gain a better understanding of the reasons for Natural Gas (NG) engine de-loading due to low LNG tank pressure.

A systematic approach was taken to find the reason behind the fall in tank pressure, which included mapping all the different sub-systems of the LNG fuel tank system influencing tank pressure. One possible factor investigated was that the Pressure Build Up (PBU) unit did not have the capacity to supply enough heat and mass through superheated gas over time to maintain the tank pressure. A literature review indicated that vapor pressure in the LNG tank will fall because of mixing of the surface layer with the bulk liquid content caused by sloshing inside the tank [1, 2]. The PBU, which acts as a vertical thermosiphon, should be able to increase the tank pressure faster than the fall in pressure from the vapor condensation resulting from the surface layer mixing. A measurement campaign was carried out on both KV Bergen and MF Korsfjord which recorded the changing conditions in the LNG tank and sub-systems before, during, and after several bunkering evolutions.

Nomenclature			Subscript	
$\dot{m}$	Mass Flow	kg/s	avg	Average
E	Energy	kJ	bulk	Bulk LNG Condition in tank
h	Enthalpy	J/kg	cond	Conduction
k	Thermal Conductivity	W/(m*K)	eff	Effective
M	Molecular Weight	g/mol	evap	Evaporation
P	Pressure	kPa	gly	Water / Glycol mixture
R	Universal Gas Constant	J/K*mol	heel	Heel, liquid
Re	Reynolds Number	-	i	Initial
S	Free Surface Area	m^2	inter	Interface
T	Temperature	K	lat	Latent Heat of Evaporation / Condensation
V	Volume	m^3	mol	Molecules (specific)
W	Power (Electric / Thermal)	kW	PBU	Pressure Build Up
y	Mole Fraction	-	sat	Saturated
ρ	Density	kg/m^3	tank	Tank

2. The fuel tank system

The goal of the measurement campaign on KV Bergen and MF Korsfjord was to find the LNG mass flow over time through the PBU to draw conclusions about tank conditions leading to natural gas engine de-loading. Fig. 1 shows the LNG tank and Vaporizer system on KV Bergen and MF Korsfjord. Both the PBU and Evaporator (EVAP) are located in the Vaporizer. In the PBU, a flow of LNG is channeled from the bottom of the LNG tank, vaporized, and led to the top of the LNG tank to maintain a certain operating pressure, 350 kPa. The EVAP channels LNG from the bottom of the LNG tank, through the Vaporizer, and to the NG engines. Waste heat from the vessel's engines is rejected in the Vaporizer through the water glycol circuit.

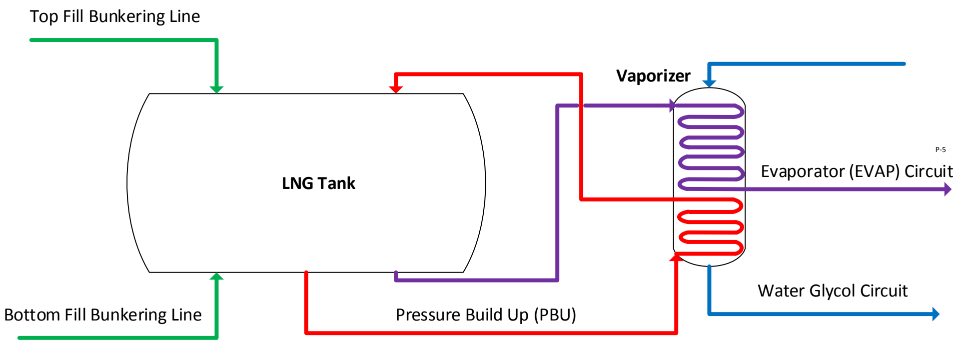

Fig. 1. Schematic of the LNG tank and Vaporizer system on KV Bergen and MF Korsfjord

3. Results

3.1. PBU Mass Flowrate

Heat and mass balances were used to relate the heat absorbed and rejected from each component in the LNG system, including the PBU, EVAP, and water glycol circuit, to determine the mass flow through the PBU. The amount of LNG circulated through the PBU is determined by the liquid height in the tank and the difference in density of the LNG. The overall heat transfer coefficient of the PBU, U, was calculated using an iterative process. The convective heat transfer occurring inside the coils of the PBU was calculated using the empirical relationships provided in [3,4,5]. The pressure change within each section of the PBU was calculated and balanced with the other sections to establish an initial estimate for the mass flow rate through the PBU. As shown in Fig. 2, section A to B is the pressure change from the top of the liquid LNG level to the inlet of the PBU. Section B to C refers to the sensible heating zone in the PBU where the LNG is brought from its sub-cooled temperature to its saturated temperature. Section C through D refers to the section of the PBU where the LNG is vaporized and superheated.

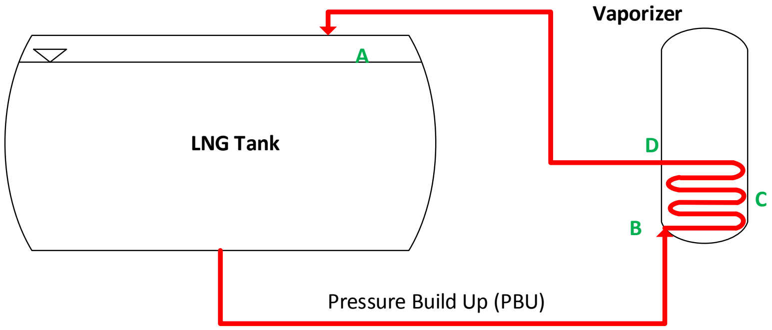

Fig. 2. Different Piping Section of the Pressure Build Up (PBU) Unit

3.2. Lowest Achievable Tank Pressure Resulting from Mixing

Before determining the required mass flow through the PBU necessary to maintain the LNG system's operating pressure, it is important to understand how mixing in the LNG causes the pressure to fall. A number of assumptions were made to calculate the lowest possible tank pressure from vapor mixing with the liquid in the LNG tank. It was assumed that complete mixing occurs between the liquid heel, LNG existing in the LNG tank before bunkering, and vapor. Mixing time was not considered and the initial vapor temperature and pressure were assumed to be 294 K and 500 kPa, respectively. The molar composition of the gas phase changes during the mixing process. The molar composition of the LNG in the tank changes very little and may be assumed constant. It was further assumed that the PBU is not affecting the pressure or temperature in the LNG tank during mixing, that there is no liquid draw from the Evaporator, and no heat leakage into the LNG tank from its surroundings. The volume occupied by the liquid and vapor does not change during mixing. After mixing, the liquid and vapor in the tank are in equilibrium at the same temperature. The effect of static liquid and vapor pressure are negligible.

The governing heat and mass equations were used to calculate the final vapor pressure after mixing. The internal energy in the LNG tank, $E_{tank,i}$, was found by considering the initial internal energy of the heel, $E_{heel,i} = (V\rho h)_{heel,i}$ and vapor, $E_{v,i} = (V\rho h)_{v,i}$, in the tank before bunkering. Equation 1 shows this basic relationship. It is important to note that the bulk heel and vapor in the tank are initially at separate temperatures before mixing, which is further explained in reference [6].

$$E_{tank,i} = (V\rho h)_{heel,i} + (V\rho h)_{v,i} \quad (1)$$

The mass in the LNG tank, $m_{tank,i}$, was found by adding the heel and vapor shown in Equation 2.

$$m_{tank,i} = (V\rho)_{heel,i} + (V\rho)_{v,i}. \quad (2)$$

The total tank volume is related to the liquid and vapor volume in Equation 3. Note that the volume in the LNG tank, V_{tank}, is a fixed value since the shape of the tank does not change.

$$V_{tank,i} = V_{heel,i} + V_{v,i}. \quad (3)$$

Using the conservation of energy, it was assumed that the heel and vapor in the tank mix completely and arrive at the same temperature after mixing. Percent liquid volume in the tank and temperature of the heel relative to the bubble point were varied to show how these two variables affect the final tank pressure after complete mixing of the tank's content. In order to illustrate how liquid sub-cooling affected final tank pressure after mixing, a reference liquid saturation temperature at a tank pressure of 500 kPa was used. At 500 kPa, the liquid bubble point temperature was calculated to be 135.9 K using the composition of LNG loaded during bunkering. Other values used in the mixing calculation include the total volume of the tank, V_{tank} at 234 m^3, initial vapor temperature $T_{v,i}$ at 294 K, and initial vapor pressure $P_{v,i}$ at 500 kPa. The initial composition of the vapor in the tank before mixing was determined using Raoult's law. Raoult's law was used instead of an Equation of State because it simplified iterative calculations [8]. The mole fraction of the LNG used to estimate the final vapor pressure after complete mixing is 0.034 N_2, 0.9149 C_1, 0.0501 C_2, 9.729E-4 C_3, 1.762E-5 C_4, and 1.917E-6 C_5.

As shown in Fig. 3, the final pressures for the range of sub-cooled liquid and percent liquid volumes used in mixing calculations always fall below the 350 kPa de-loading pressure. These results suggest that if the content of the LNG tank is completely mixed then the tank pressure will fall below the lowest tank pressure the LNG system can handle causing a de-loading event. It may be inferred that NG engine de-loading can result from liquid and vapor mixing in the tank. It is uncertain, however, how much of the liquid and vapor mix with one another in different situations.

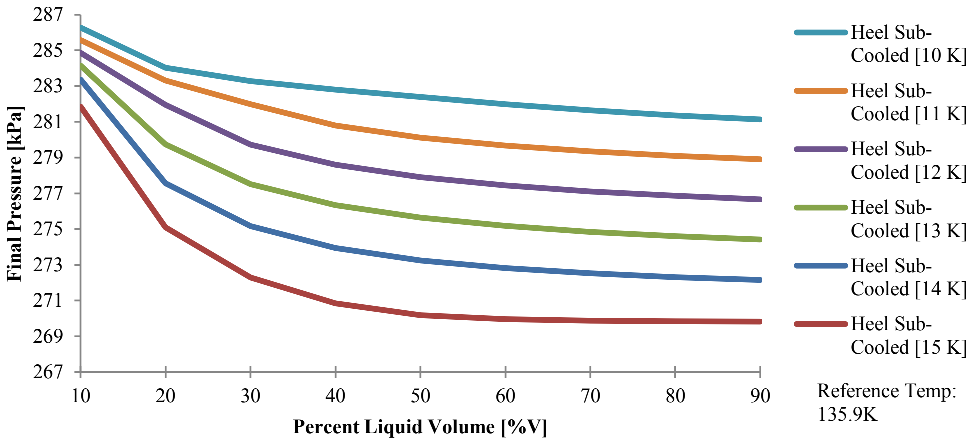

Fig. 3. Final Tank Pressure After Complete Liquid and Vapor Mixing Given Different Initial Liquid Temperatures

A measurement campaign was defined to find actual values to relevant parameters. Since the instrumentation on board was not measuring many of the relevant parameters, additional measurements had to be made and special procedures had to be implemented.

3.3. Initial Fuel Tank Temperatures

The "instrument flush method" was employed to measure the liquid heel temperature of the LNG in the tank. Two K-type thermocouples were attached to the outside of the bottom instrument piping. Heavier hydrocarbons (natural gas liquids), which build up in this piping, are flushed by pushing LNG from the bottom of the tank to the mast. Flashing and corresponding errors in temperature measurement were avoided by placing the thermocouples as close to where the piping met the tank as possible. The entire duration of the instrument flush was 159 seconds and the lowest pipe surface temperature recorded was -148.75°C (124.25 K). This measurement indicates the liquid heel temperature in the LNG tank before mixing.

A "vapor purge method" was employed to try to measure the liquid surface layer temperature in the LNG tank on KV Bergen and MF Korsfjord. Before bunkering, the hose connecting the bunkering station or truck to the vessel receiving LNG is inerted with nitrogen first and then NG from the top of the LNG tank on the vessel. The piping used in this process is shown as the "Top Fill Bunkering Line" in Fig. 1. During top tank vapor purging, the vapor pressure is brought down to a saturated state which corresponds to the liquid surface temperature [6, 7]. The lowest pressure achieved in the tank during purging was 4.719 bara which corresponds to a liquid saturation temperature of -138.9°C. A separate measurement was taken to find the average temperature of LNG entering the LNG tank on the ship during bunkering. During the measurement, bunkering occurred entirely from the top of the LNG tank through the “Top Fill Bunkering Line”. An asymptotic liquid bunkering temperature of -153.6°C was recorded. This measurement indicates the liquid bunkering temperature delivered to the LNG tank on the vessel.

After bunkering, MF Korsfjord was allowed to remain at the pier for several hours while the bunkered LNG introduced above the heel in the tank was allowed to mix. During this period, a fall in tank pressure was observed. The tank pressure reached a steady state value of 282.84 kPa after the heel and bunkered LNG finished mixing.

3.4. Evaporator (EVAP) Measurements

In order to calculate the heat absorbed by LNG traveling through the EVAP (see Fig. 1.), the temperature of the LNG entering the EVAP, NG exiting the EVAP and mass flow through the EVAP are required. The mass flow rate through the EVAP was calculated by using a correlation between the power produced by the NG engines giving the total amount of fuel consumed by both engines.

As expected, the curve for the heat absorbed in the EVAP in Fig. 4 resembles the power produced by the NG engines over time. While maneuvering away from the pier more power is required resulting in a spike in load on the NG engines and heat absorbed by the EVAP (e.g. minute 38 to 41). This spike is followed by a relatively constant load placed on both engines while MF Korsfjord is transiting (e.g. minute 41 to 57) and finally a short period of low load on the engines while the vessel idles alongside the pier (e.g. minute 57 to 66).

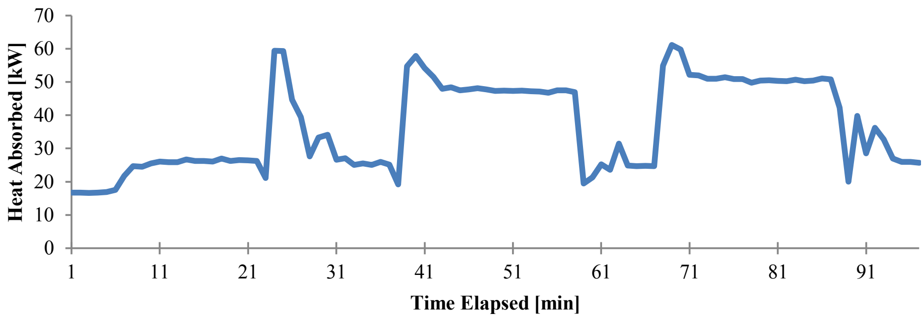

Fig. 4. Heat Absorbed by the Evaporator while MF Korsfjord Transits

3.5. PBU Mass Flow

The mass flow circulated through the PBU (see Fig. 1.) was calculated using a heat balance of the heat being absorbed and rejected in the Vaporizer. The heat absorbed by the PBU is calculated using a simple heat balance of the different streams entering and leaving the Vaporizer. Equation 4 was used to calculate the heat absorbed by the PBU together with the measurements conducted in [8]. Fig. 5 illustrates the relationship between the different heat streams. Terms which were not included in Equation 4 were the heat leakage from the Vaporizer to the surroundings and any frost solidification which may form on the coils of the PBU or EVAP. Since these two terms were neglected in calculations, Fig. 5 shows situations where the combined heat absorbed by the EVAP and PBU are greater than the heat rejected in the Vaporizer found by the temperature measurements and may account for the heat leakage and frost formation neglected, the latter being more important.

$$W_{gly} = W_{PBU} + W_{EVAP} \tag{4}$$

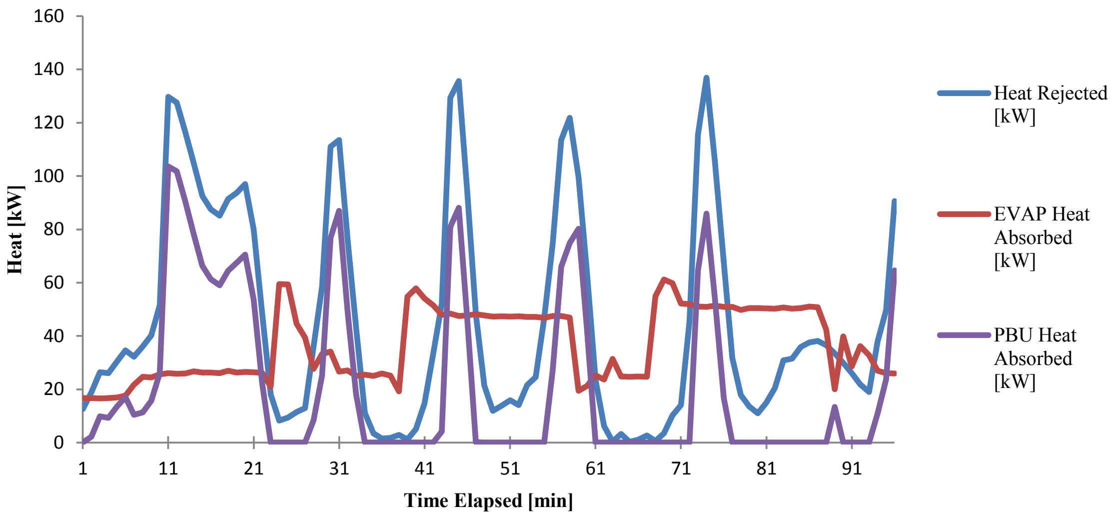

Fig. 5. Heat Exchange between the Water Glycol (Heat Rejected), EVAP and PBU (Heat Absorbed) in the Vaporizer based on measurements onboard MF Korsfjord

Fig. 6 shows the measured PBU value opening and the corresponding mass flow rate while the PBU valve is open.

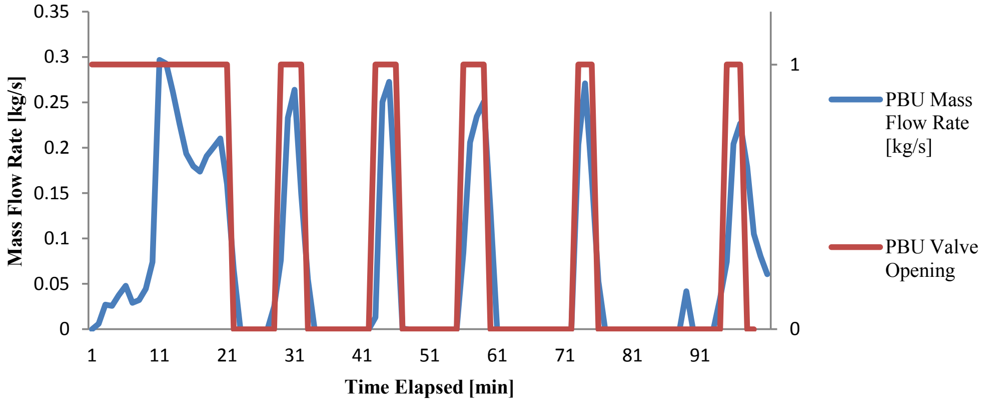

Fig. 6. Heat Exchange between the Water Glycol (Heat Rejected), EVAP and PBU (Heat Absorbed) in the Vaporizer

The average PBU mass flow rate was calculated by dividing the total mass of LNG circulated through the PBU by the PBU valve opening time and found to be 0.16 kg/s.

4. Analysis and Discussion

After calculating mixing conditions which cause NG engine de-loading and measuring the PBU mass flow rate during vessel maneuvering, steps were taken to find what LNG system conditions cause NG engine de-loading.

4.1. Rate of Vapor Condensation

The mass rate of vapor condensation must be found in a still tank to establish a baseline for how much vapor is condensed when the PBU is operating. A comparison of the idealized pressurization time with the actual pressurization time in the tank suggests that vapor condensation occurs while vapor exiting the PBU builds tank pressure. Only a portion of the superheated vapor supplied to the top of the tank by the PBU remains in vapor form. The mass rate of vapor retained in the vapor section, $\dot{m}_v$, may be illustrated by a simple mass balance shown in Equation 5. The process used for calculating vaporization times is found in [8].

$$\dot{m}_v = \dot{m}_{PBU} - \dot{m}_{cond} \tag{5}$$

Using different vapor condensation rates, a range of pressurization times were calculated. Fig. 7 illustrates how the pressurization time changes as the rate of condensation varies. In Fig. 7, the percent (%) condensation refers to mass percent of vapor coming from the PBU which condenses again. In this illustration, 100% indicates that all LNG vaporized in the PBU is condensed again with no effect on the pressure in the LNG tank. It was determined that when 66.2% of the PBU mass flow rate condensed, the calculated pressurization time deviated no more than 3.6% of the actual tank pressure versus time for Experiment E1, and no more than 3.2% for Experiment E2, conducted on MF Korsfjord. This suggests that approximately 0.106 kg/s of vapor condenses while the tank is un-disturbed. Using the values for an un-disturbed tank, the thickness of the liquid surface layer may be estimated.

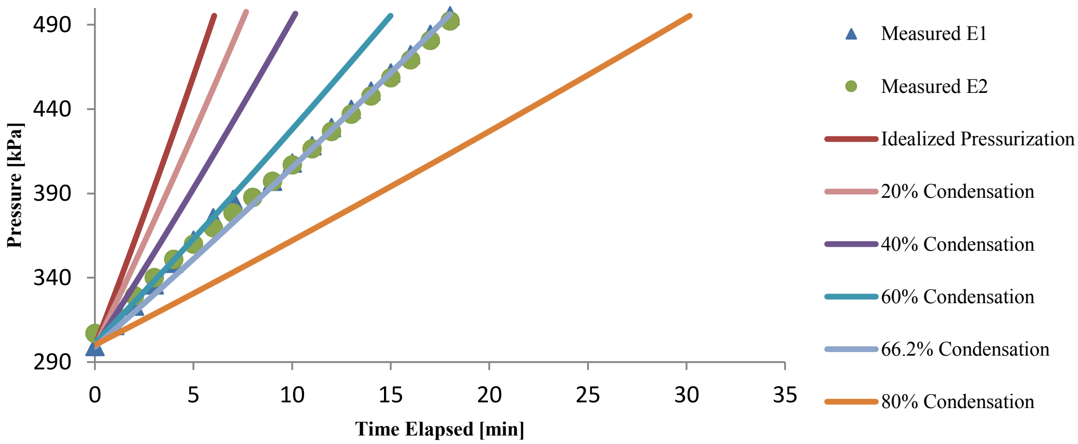

Fig. 7. LNG Tank Pressurization Time with Vapor Condensation

Using the rate of vapor condensation during PBU operation, it is possible to determine the thickness of the liquid surface layer between the bulk liquid and vapor section described in [1,2,6,7].

4.2. Vapor Condensation during Disturbed Conditions

To determine the rate of vapor condensation and de-loading time under different mixing conditions, the thickness of the surface layer of an undisturbed tank is estimated to provide a base case. A modified version of Fourier's Law, provided in Equation 6, may be used to calculate the heat transfer occurring in the thin surface liquid vapor region in the LNG tank. Equation 6 assumes that the conductive and convective heat transfer occurring in the liquid surface may be shown as a layer of effective conduction. The thickness of this effective conduction layer on the liquid surface is shown in Equation 6 as $x_{eff,cond}$. Similar to [6,7], the effective thermal conductivity coefficient, $k_{eff,cond}$, may be used to account for conduction and convection occurring in the liquid surface. It is also assumed that only latent heat is rejected from the vapor section to the surface sub-layer. Sensible heat rejected by the superheated vapor is neglected to simplify the calculation.

$$W_{cond,eff} = \left[\frac{k_{eff,cond} S\left(T_{sat}\left(P_{v,i}\right) - T_{bulk}\right)}{x_{eff,cond}}\right] \tag{6}$$

Equation 7 reflects the assumption that only latent heat rejected by vapor during condensation is absorbed by the liquid surface layer.

$$W_{cond,eff} = \dot{m}_{cond} h_{lat} \tag{7}$$

The effective thickness of the surface layer may be calculated by combining Equation 6 and Equation 7. The initial values and estimated surface layer thickness is found in Table 1. The effective thermal conductivity, $k_{eff,cond}$, comes from [6]. The flat liquid vapor interface area is the longitudinal cross section area of the LNG tank on MF Korsfjord. A vapor pressure, $P_{v,i}$, reflects the desired LNG tank pressure during operations with a corresponding liquid bubble point temperature, $T_{sat}\left(P_{v,i}\right)$. The bulk liquid temperature, T_{bulk}, and latent heat of condensation, h_{lat}, was determined in [8] and the rate of condensation, $\dot{m}_{cond}$, was determined from a heat and mass balance of the LNG system. Finally, the effective surface layer thickness, $x_{eff,cond}$, was calculated from Equations 6 and 7.

Table 1. Effective Undisturbed Liquid Surface Layer Parameters

Parameter	Symbol	Value	Unit
Effective Thermal Conductivity	$k_{eff,cond}$	0.275	W/mK
Vapor Pressure	$P_{v,i}$	500	kPa
Flat Liquid Vapor Interface Area	S_{flat}	44.21	m^2
Liquid Bubble Point Temperature	$T_{sat}\left(P_{v,i}\right)$	134.9	K
Bulk Liquid Temperature	T_{bulk}	120.99	K
Rate of Condensation	$\dot{m}_{cond}$	0.16	kg/s
Latent Heat of Condensation	h_{lat}	579	kJ/kg
Effective Surface Layer Thickness	$x_{eff,cond}$	1.83	mm

Using the undisturbed surface layer thickness and vapor liquid interface area, the two values may be varied to illustrate how the rate of condensation in the tank changes. As shown in Equation 6, when the thickness of the effective surface layer decreases, the rate of heat transferred through the effective conduction region increases. This causes the rate of condensation to increase. Similarly, when the liquid vapor interface area increases, the rate of condensation also increases, which may correspond to a wavy surface. Further analysis must be conducted to show how changing the thickness of the liquid surface layer and liquid surface area will lead to falling LNG tank pressure and potentially NG engine de-loading.

5. Conclusion

This study has shown that it is possible to cause NG engine de-loading by mixing the liquid and gas contents of an LNG tank on a LNG fueled vessel. Measurements were conducted onboard two vessels to determine realistic values for different components in the vessels' LNG fuel system. A model for calculating the effective condensation rate was introduced, as well as a baseline for condensation in an undisturbed fuel tank. Further analysis should determine how the vessel's motion causes mixing inside the LNG tank, resulting in increased condensation rate of the vapor pillow above the LNG. Focus should be placed on how the sloshing motion inside the tank may erode the liquid surface layer. Ultimately, it would be useful for LNG tank manufacturers to understand what sloshing characteristics cause the LNG tank pressure to fall below an acceptable limit causing NG engine de-loading.

6. References

[1] Moran, M., McNelis, N., Kudlac, M., Haberbusch, M., & Satornino, G. (1994). *Experimental Results of Hydrogen Slosh in a 62 Cubic Foot (1750 Liter) Tank* Paper presented at the 30th Joint Propulsion Conference Indianapolis, Indiana.

[2] Ludwig, C., Dreyer, M. E., & Hopfinger, E. J. (2013). Pressure variations in a cryogenic liquid storage tank subjected to periodic excitations. *International Journal of Heat and Mass Transfer, 66*(0), 223-234. doi: http://dx.doi.org/10.1016/j.ijheatmasstransfer.2013.06.072

[3] Patil, R., Shende, B. , & Ghosh, P. (1982). Designing a Helical-Coil Heat Exchanger *Chemical Engineering*

[4] Kern, D. (1950). *Process Heat Transfer*. New York: McGraw-Hill.

[5] Gnielinski, V. (1987). Critical Reynold's Number of Helically Coiled Tubes Heat Exchanger Design Handbook (2nd Ed.) Hemisphere Publishing

[6] Scurlock, R.G. (2006). *Low-Loss Storage and Handling of Cryogenic Liquids: The Application of Cyogenic Fluid Dynamics*: Kryos Publications.

[7] Scurlock, R. G. (1988). Cryogenics at the University of Southampton: a review. *Cryogenics, 28*(7), 439-466. doi: http://dx.doi.org/10.1016/0011-2275(88)90112-9

[8] Direnzo, J. (2014). Investigation of an LNG fuel system for a Norwegian Coast Guard Ship. Norwegian University of Science and Technology. http://urn.kb.se/resolve?urn=urn:nbn:no:ntnu:diva-25838